JOC The Journal of Organic Chemistry

ARTICLE

pubs.acs.org/joc

Solution Processable Indoloquinoxaline Derivatives Containing Bulky Polyaromatic Hydrocarbons: Synthesis, Optical Spectra, and Electroluminescence

Payal Tyagi, A. Venkateswararao, and K. R. Justin Thomas*

Organic Materials Lab, Department of Chemistry, Indian Institute of Technology Roorkee, Roorkee 247 667, India

Supporting Information

ABSTRACT: New hybrid materials featuring the dipolar fragment 6*H*-indolo[2,3-*b*]quinoxaline attached to the bulkier polyaromatic hydrocarbons such as fluoranthene, triphenylene, or polyphenylated benzene have been synthesized by a two-step procedure involving Sonogashira and Diels−Alder reactions. They were characterized by absorption, emission, electrochemical, thermal, and theoretical investigations. The electronic properties of the compounds were dominated by the 6*H*-indolo[2,3-*b*]quinoxaline chromophore, and the incorporation of polyaromatic hydrocarbons reduces the chances of nonradiative deactivation processes associated with the excited state and improves the emission properties. The compounds displayed cyan emission with moderate quantum efficiency when excited at the absorption maximum. All of the compounds exhibited an irreversible reduction process corresponding to the addition of electron at the quinoxaline segment. They showed moderate thermal stability and glass transition temperature greater than 100 °C. The presence of rigid 6*H*-indolo[2,3-*b*]quinoxaline and bulkier polyaromatic hydrocarbon segments enhances the thermal stability and glass transition temperature significantly. Finally, the dyes were successfully applied as an electron-transporting and emitting layer in multilayered organic light-emitting diodes comprising a *N*,*N*′-bis(l-naphthyl)-*N*,*N*′-diphenyl-1,1′-biphenyl-4,4′-diamine hole-transporting layer. The cyan emitting devices were characterized by moderate device performance parameters.

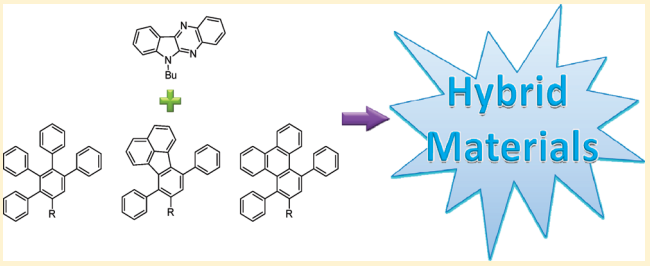

INTRODUCTION

Functional materials derived from polyaromatic hydrocarbons such as fluorene,[1] anthracene,[2] pyrene,[3] perylene,[4] triphenylene[5] and fluoranthene[6] have been intensively studied in recent years due to their promising emission thermal and charge transport properties. They are widely used as emitters in organic light-emitting diodes, semiconducting constituents in thin-film transistors, reporters in fluorescent sensors and π-conjugating chromophores in nonlinear optical materials. As a result of their extended conjugation and rigidity, they display strong emission with relatively low Stokes shifts. However, because of the planar structure, they are prone to stronger intermolecular $\pi-\pi$ stacking interactions, which often reduce their luminescence and increase the propensity to form crystals in the solid state.[7] Although the stacking interactions are beneficial for charge transport properties, crystallinity and reduction in emission yield or unwanted red-shift in emission in the solid state poses a severe problem in the utilization of polyaromatic hydrocarbon derived materials in organic light-emitting diodes.[8]

One of the answers to the above-mentioned problem is the introduction of bulkier and nonplanar structural elements in the polyaromatic hydrocarbon core. For instance, substitution of *tert*-butyl groups on anthracene hinders the stacking interactions.[9] Similarly, the polyarylated polyaromatic hydrocarbons have also been demonstrated to resist the close proximity of the molecules in the solid state due to their twisted structure.[10] Interest in polyaromatic hydrocarbons containing arylamines stemmed partially from their bright red-shifted emission and favorable hole-transport properties when compared to the parent systems.[6] Arylamine substituted polyaromatic hydrocarbons have also been found to suppress the close molecular association and lead to improved emission and hole-transport properties.[10] Polyphenylated phenylene dendrons anchored on low-band gap chromophores such as benzothiadiazole have been developed to achieve red emission and dual transport properties.[11] In addition, the polyphenylated aromatic cores serve as a platform for the disposition of electron-donating and -accepting chromophores in precise locations and pave the way for the tuning of donor−acceptor interactions. Even though many polyaromatic hydrocarbons and their derivatives have been exploited for applications in electro-optics, their heteroaromatic analogues remain scarce.[12]

Earlier, we have reported the synthesis and characterization of amine substituted indoloquinoxaline derivatives whereby we observed that the nature of the conjugation connecting the amine unit with the indoloquinoxaline segment is more important than the nature of the aryl substituents on the amino group

Received: March 4, 2011
Published: May 03, 2011

to alter the absorption and emission characteristics.[13] The emission of the amine-substituted derivatives was quenched due to the presence of strong intramolecular dipolar interactions. In an attempt to improve the emission properties of the molecular materials derived from the 6*H*-indolo[2,3-*b*]quinoxaline fragment, we have attached bulkier and nonplanar multiply substituted polyaromatic hydrocarbons to the indole nucleus. As there are no strong electron donors in these structures, they have exhibited bright luminescence and opened avenues for applications in electroluminescent devices as emitting and electron-transporting materials. In this report, we present the synthesis and characterization of 6*H*-indolo[2,3-*b*]quinoxaline-based Müllen dendron-like[14] molecular materials (Chart 1) and their function as emitting and electron-transporting components in double layer organic light-emitting diodes.

Chart 1. Structures of Polyaromatic Hydrocarbons (PAHs) Containing Indoloquinoxaline Moiety

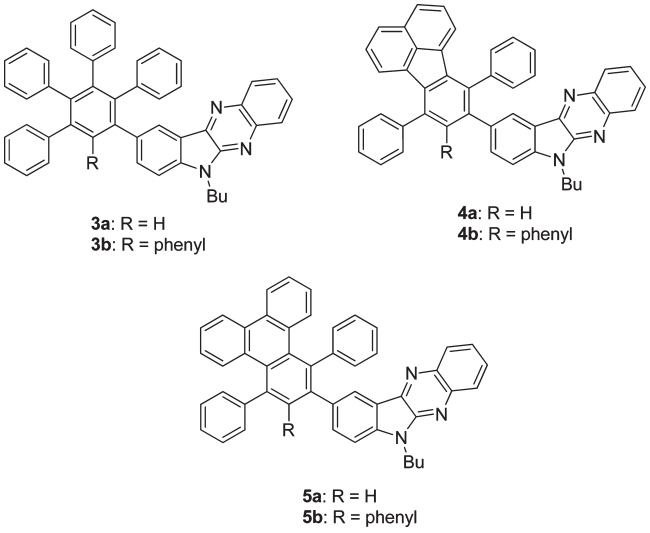

RESULTS AND DISCUSSION

Synthesis and Characterization. The structures of the compounds synthesized in this study are presented in Chart 1. The synthetic routes used for the preparation of the new materials are shown in Scheme 1. These compounds were easily obtained by the Diels–Alder reaction between the suitably substituted cyclopentadienones and indoloquinoxaline based acetylenes followed by decarbonylation. The acetylenes required for the synthesis were obtained by the Sonogashira coupling

Scheme 1. Synthetic Route to the Compounds

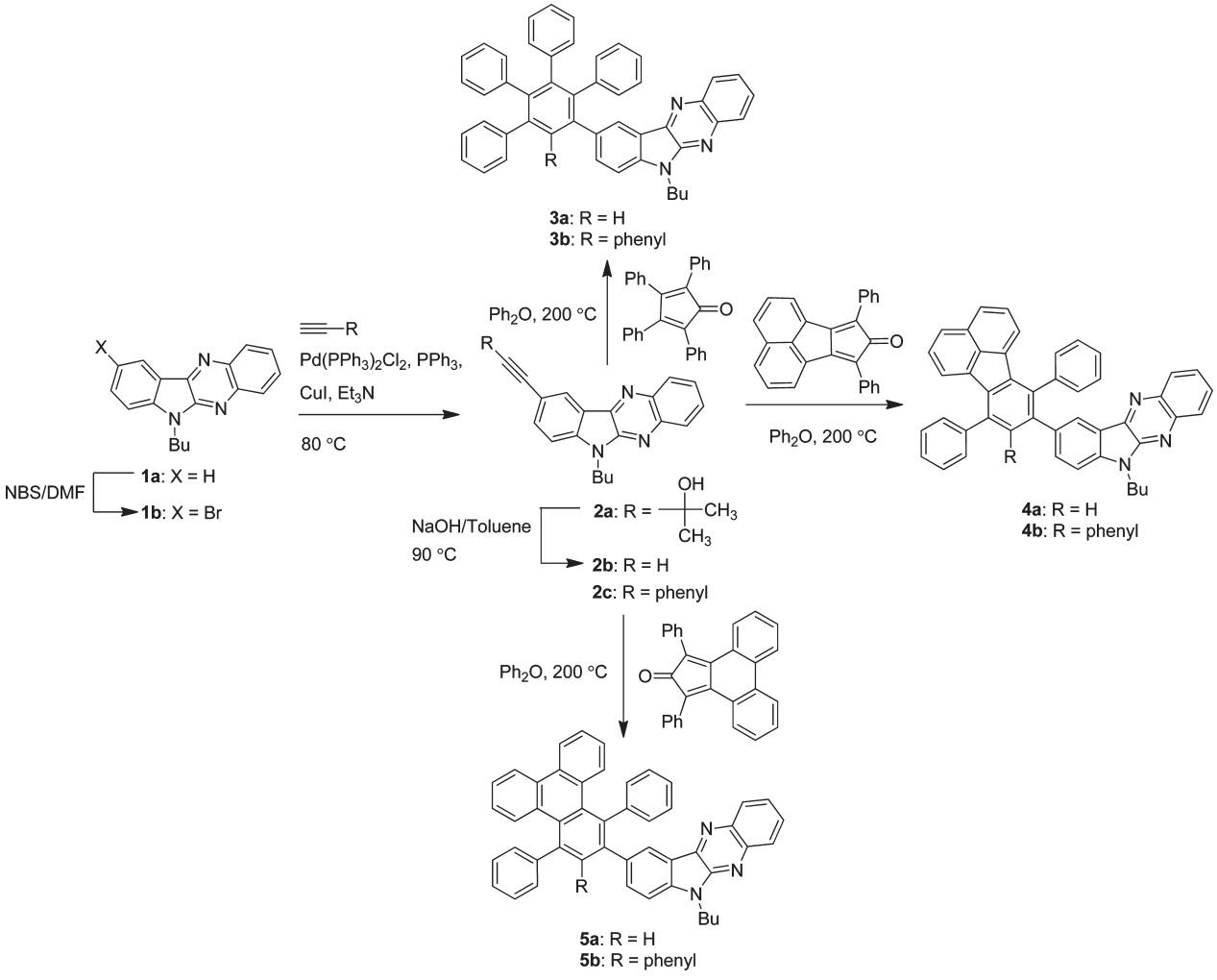

dx.doi.org/10.1021/jo2004764 |*J. Org. Chem.* 2011, 76, 4571–4581

Table 1. Photophysical Properties of Compounds 3a–5b

	dichloromethane			toluene			
compd	λ_{max}, nm (ε_{max}, M^{-1} cm^{-1} × 10^3)	λ_{em}, nm (Φ_f)[a]	Stokes shift, cm^{-1}	λ_{max}, nm (ε_{max}, M^{-1} cm^{-1} × 10^3)	λ_{em}, nm[a] (Φ_f)	Stokes shift, cm^{-1}	λ_{em}, nm[b]
3a	264 (46.0), 291 (42.6), 344 (17.6), 359 (23.2), 414 (4.4)	501 (0.15)	4195	411 (4.0), 358 (24.8), 342 (18.8), 290 (43.9)	477 (0.15)	3367	498
4a	271 (37.1), 290 (43.2), 300 (45.4), 331 (21.8), 360 (31.8), 413 (7.4)	506 (0.14)	4450	360 (32.8), 344 (23.7), 332 (22.6), 301 (44.2)	483 (0.14)	3686	499
5a	273 (60.8), 295 (61.6), 342 (30.6), 360 (31.9), 415 (4.6)	499 (0.15)	4056	360 (4.4), 294 (9.2)	480 (0.15)	3557	485
3b	273 (43.3), 289 (39.8), 344 (17.7), 360 (23.8), 413 (3.8)	504 (0.16)	4372	410 (3.9), 360 (25.5), 342 (18.6), 288.5 (40.2)	476 (0.17)	3382	494
4b	276 (44.6), 289 (53.3), 331 (18.5), 345 (23.5), 361 (34.2), 416 (4.9)	500 (0.17)	4039	360 (16.3), 288 (22.5)	487 (0.17)	3856	482
5b	276 (72.6), 286 (71.9), 344 (23.0), 361 (27.8), 409 (4.6)	503 (0.02)	4569	411 (4.0), 360 (28.5), 342 (23.8), 286 (65.5)	485 (0.16)	3712	494, 559

[a] Quantum yield measured relative to coumarin-6. [b] Measured for thin film.

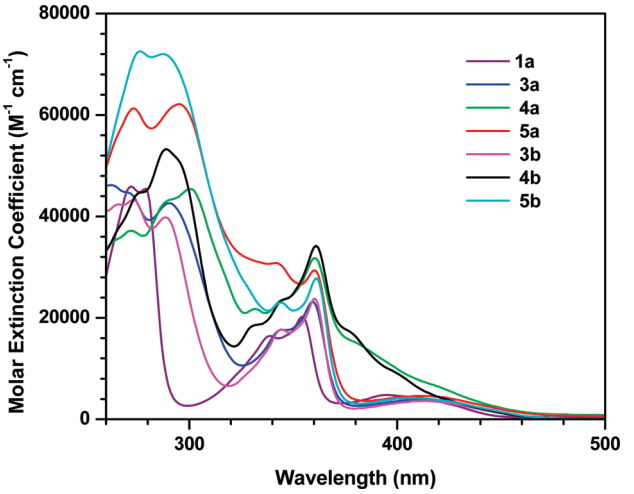

Figure 1. Absorption spectra of the compounds recorded in dichloromethane.

reaction[15] of 9-bromo-6-butyl-6*H*-indolo[2,3-*b*]quinoxaline (**1b**) with a corresponding terminal acetylene. All target compounds (**3**, **4**, and **5**) were characterized by NMR spectroscopy, mass spectrometry, and elemental analysis. The compounds are yellow in color and reasonably soluble in solvents such as dichloromethane, tetrahydrofuran, toluene, etc. and insoluble in alcohols. The dilute solutions of the dyes appear yellow and fluoresce in the cyan region. The analytically pure samples were used for the electro-optical investigations.

Photophysical Properties. The photophysical behavior of the compounds has been examined by measuring absorption and fluorescence spectra in five different solvents, *viz.*, cyclohexane (ch), toluene (tol), tetrahydrofuran (thf), dichloromethane (dcm) and acetonitrile (acn). The pertinent data are compiled in Table 1 and Table S1 (Supporting Information). The absorption spectra recorded for the dyes in dichloromethane are displayed in Figure 1. For comparison, the absorption spectrum of the parent compound, 6-butyl-6*H*-indolo[3,2-*b*]quinoxaline (**1a**) is also shown.

All of the compounds exhibit a well-resolved absorption profile in the range of 250−460 nm. Invariably all of the compounds show four absorption envelopes at ∼270, ∼340, ∼360 and ∼410 nm, respectively. Since these peaks are present in the parent compound, 6-butyl-6*H*-indolo[3,2-*b*]quinoxaline (**1a**), they are assigned to the indoloquinoxaline localized electronic excitations.[13] Among these four transitions, the three higher energy absorptions are probably originating from the $\pi-\pi^*$ and $n-\pi^*$ transitions, while the lower energy band is attributed to the charge transfer transition between the indole and quinoxaline segments. The mediocre intensity observed for the charge transfer transition indicates a poor orbital overlap. Such a weak charge transfer transitions are also reported for fused donor−acceptor compounds such as thienopyrazines.[16]

Additionally, all of the compounds exhibit an intense absorption peak at 286−300 nm due to the aryl core of the Müllen dendron-like structure. The intensity of this band increases in the order benzene < fluoranthene < triphenylene. The increase in extinction coefficient for this band is probably attributed to the progressive extension in conjugation on moving from benzene to triphenylene. Extended delocalization of π-electrons over a large area of a molecule is expected to broaden the absorption band

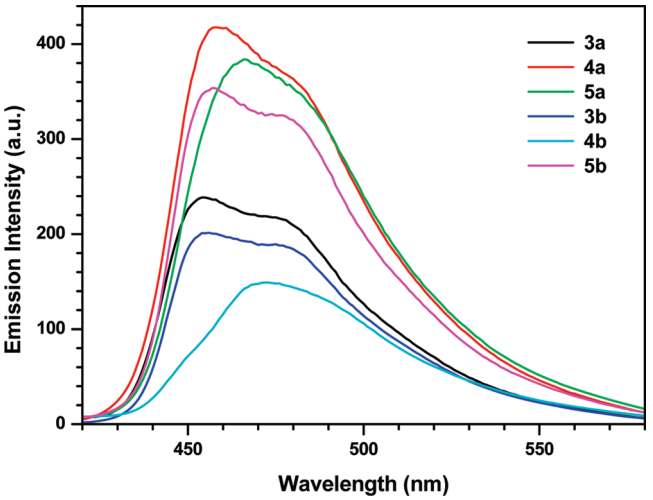

Figure 2. Fluorescence spectra of compounds **3**, **4**, and **5** recorded in cyclohexane.

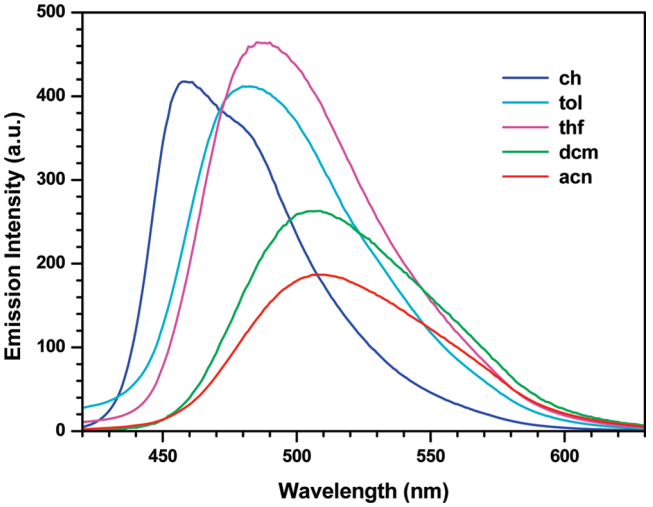

Figure 3. Emission spectra of **4a** recorded in different solvents.

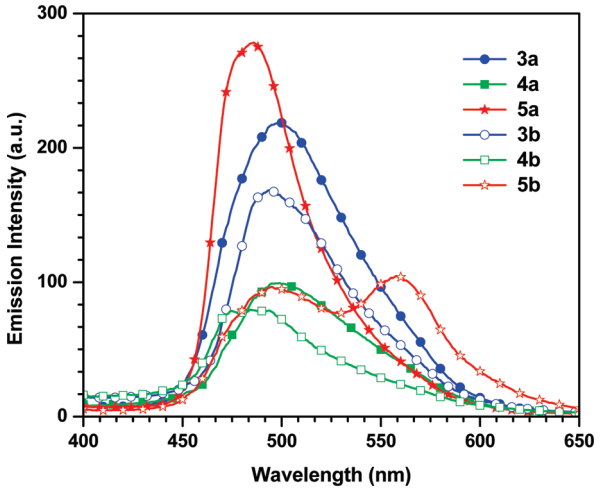

Figure 4. Fluorescence spectra of the compounds recorded for the spin-coated films.

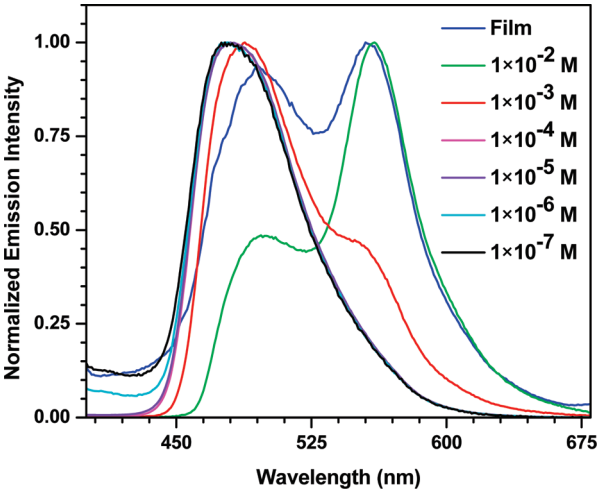

Figure 5. Emission spectra of the compound **5b** recorded for the spin-coated film and at various concentrations in toluene.

and increase optical density.[17] For the triphenylene based dyes **5a** and **5b**, the absorption peaks appear at shorter wavelength (295 and 286 nm) when compared to those containing fluoranthene cores (**4a** and **4b**) (300 and 289 nm). From this it is clearly evident that the fluoranthene segment has a slightly lower $\pi-\pi^*$ transition energy than the triphenylene analogue.[18]

A bright bluish green emission is observed for all of the derivatives in cyclohexane (Figure 2). This underwent a pronounced bathchromic shift on increasing the polarity of the solvent as illustrated for compound **4a** in Figure 3. The most red-shifted emission for the each dye was observed for acetonitrile solutions with substantial reduction in the fluorescence quantum efficiency. These solvent-dependent emission charecteristics are more likely to stem from the difference in the dielectric constant of the medium, which would result in a more efficient solvation in the excited state.[19] Also, the excited state appears to be more polar than the ground state in view of the large Stokes shifts observed for these compounds (Table 1). A reasonably large Stokes shift is also desirable for the application in electroluminescent devices as it ensures the reduction of self-absorption.

As solid films all of the compounds emit with appreciable intensity (Figure 4), and the emission maxima for the films are located between those observed for toluene and dichloromethane solutions with the exception of compound **5b**. For instance, **5a** displays a blue-shifted emission profile in solid film (485 nm) when compared to that observed for dichloromethane solution (499 nm). This suggests that the dielectric constant for the solid films of the compounds lies close to that in tetrahydrofuran and less than that in dichloromethane.[20] However, for the solid film of **5b** two bands were observed with a green emission band centered at 494 nm and a yellow emission band peaking at 559 nm. Since the higher energy band is similar to the emission band noticed in dilute dichloromethane solution, it can be assigned to the monomer emission of compound **5b**. To identify the nature of the dual emission observed for compound **5b**, the emission spectra of **5b** in toluene with different concentrations were measured by exciting at 360 nm. The spectra recorded in different concentrations are shown in Figure 5 along with the photoluminescence spectrum of the solvent cast thin film. On increasing the concentration, the intensity of the

dx.doi.org/10.1021/jo2004764 |J. Org. Chem. 2011, 76, 4571–4581

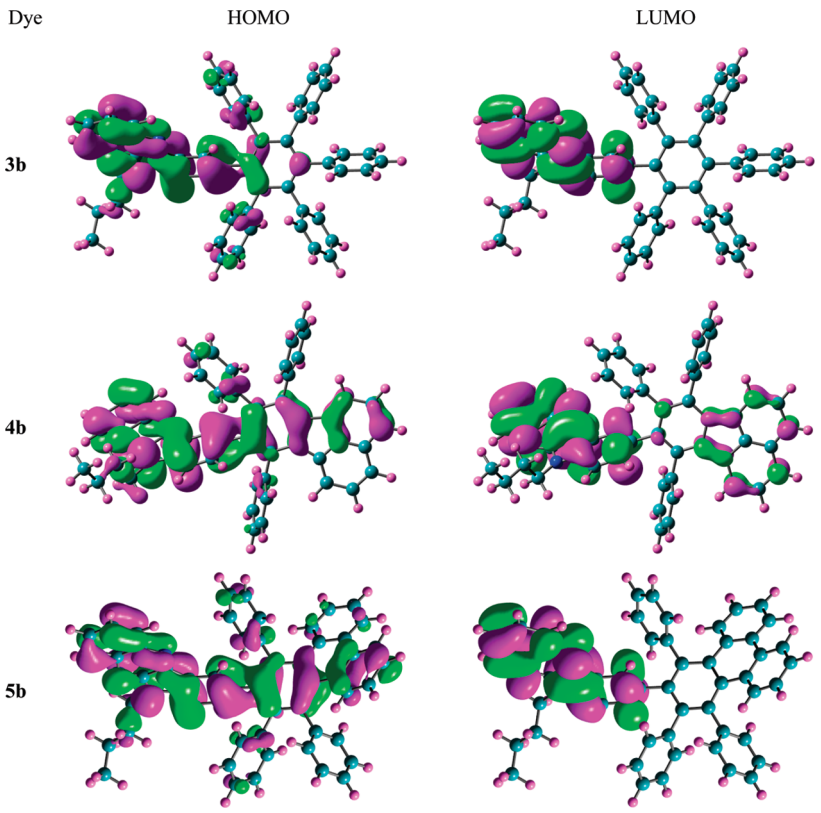

Figure 6. Frontier molecular orbitals of the dyes computed by using TDDFT at the B3LYP level.

emission band at 494 nm decreases and a new band at 559 nm gradually appears. The higher wavelength emission band starts appearing at a concentration of 1×10^{-3} M. At higher concentrations, probably the molecular aggregation takes place, leading to excimer formation. It is possible that the excimers emit in the red-shifted wavelength when compared to the monomer.[21] It is interesting to observe aggregation resulting from $\pi-\pi$ interactions despite the presence of twisted aryl substituents. The $\pi-\pi$ stacking interactions between the triphenylene moieties leading to columnar structures have been well documented in the literature, and this behavior was found to be responsible for their special liquid-crystalline properties.[22] It is to be noted here that aggregation-induced emission, once considered as detrimental for electroluminescence, has been exploited for applications such as chemosensors and favorable charge transporting as long as there is no aggregation-induced quenching.[23]

To understand the electronic structure of the compounds, TDDFT calculations were performed on **3b**−**5b** using the Gaussian 09 package.[24] Figure 6 shows the theoretically computed molecular orbitals in the ground states for compounds **3b**, **4b** and **5b**. In all of the compounds the HOMO and LUMO are mainly constituted by the indoloquinoxaline segment. This clearly demonstrates that the HOMO to LUMO transition occurring in these compounds at higher wavelength with low optical density is originating from the indoloquinoxaline unit. However, in the case of **4b** and **5b** the HOMO is spread over the fluoranthene and triphenylene segments, respectively, which explains the perturbations seen in the higher wavelength absorption for these compounds. The energies of the HOMO and LUMO levels and the ground state dipole moment computed for the dyes (**3b**−**5b**) are also collected in Table 2. The frontier orbital energies remain the same for all of the compounds, which is consistent with the values deduced from the electrochemical results (*vide supra*). This shows that the frontier orbitals are derived from the same chromophore in all three compounds.

Vertical transitions for compounds **3b**−**5b** were calculated by employing the TDDFT method. The transition energies, oscillator strengths, and assignments for the most relevant singlet excited states in the each molecule are listed in Tables 2. The theoretically computed gas phase low energy vertical transitions match well with the values realized for the compounds in dichloromethane solutions. As the compounds have not shown any solvatochromism in the ground state (see Supporting Information for absorption spectra recorded in toluene solutions), it is likely that the solvents play a less significant role in the absorption profiles of the present compounds. The striking resemblance of the experimental optical parameters to the theoretically computed values using TDDFT and B3LYP/6-31(d,p) is interesting to note here as the donor−acceptor compounds are generally believed to show deviations from TDDFT predictions at the B3LYP level. The next higher energy transitions occurring in the range 330−360 nm are composed of several electronic excitations such as HOMO-1 to LUMO, HOMO-1 to LUMO+1, and HOMO-3 to LUMO.

Electrochemical Properties. The redox propensity of the materials is a crucial factor that affects the performance of the OLEDs fabricated using them, as it will exert a direct impact on the charge injection and mobility in the molecular layer.[25] We have examined the redox behavior of the compounds by the cyclic voltammetric and differential pulse voltammetric methods in dichloromethane solutions. The potentials are reported relative to the internal standard, ferrocene. All of the molecules

dx.doi.org/10.1021/jo2004764 |*J. Org. Chem.* 2011, 76, 4571–4581

Table 2. Computed Vertical Excitation Energies, Dipole Moments, and Frontier Orbital Energies for Dyes 3b−5b

compd	λ_{max}, nm	f	assignment	μ_g, D	HOMO, eV	LUMO, eV
3b	407.2	0.025	HOMO → LUMO (97%)	2.18	−5.42	−1.80
	336.3	0.065	HOMO-1 → LUMO (95%)			
	328.4	0.242	HOMO-3 → LUMO (83%)			
	299.3	0.297	HOMO → LUMO+1 (88%)			
	294.6	0.124	HOMO → LUMO+2 (82%)			
4b	408.7	0.039	HOMO → LUMO (93%)	2.20	−5.39	−1.81
	386.0	0.047	HOMO → LUMO+1 (78%)			
	362.7	0.194	HOMO-1 → LUMO (47%)			
			HOMO-1 → LUMO+1 (29%)			
	328.5	0.256	HOMO-3 → LUMO (83%)			
5b	409.5	0.026	HOMO → LUMO (95%)	2.52	−5.41	−1.83
	330.0	0.345	HOMO-4 → LUMO (48%)			
			HOMO-3 → LUMO (37%)			

Table 3. Electrochemical and Thermal Data of the Compounds

compd	E_{red}, mV[a,b]	LUMO, eV[c]	HOMO, eV[d]	E_{0-0}, eV[e]	T_g, °C[f]	T_{onset}, °C[g]	T_d, °C[h]	T_c, °C[i]	T_m, °C[j]
3a	−2110 (i)	2.69	5.36	2.67	103	400	491		
4a	−2100 (i)	2.70	5.37	2.67	116	363	494		303
5a	−2100 (i)	2.70	5.37	2.67		450	492	232	359
3b	−1990 (i)	2.81	5.48	2.67	135	414	491	207	319
4b	−2120 (i)	2.68	5.35	2.67		460	483		
5b	−2130 (i)	2.67	5.34	2.67	156	465	496		

[a] Measured in dichloromethane. [b] Obtained from differential pulse voltammograms. Potentials reported are referenced to the ferrocene internal standard. [c] Derived from reduction potential using $E_{LUMO} = 4.8 + E_{red}$. [d] Deduced using the formula $E_{HOMO} = E_{LUMO} + E_{0-0}$. [e] Calculated from the optical edge measured for dichloromethane solution. [f] Glass transition temperature obtained from differential scanning calorimetry. [g] Temperature corresponding to 5% weight loss. [h] Decomposition temperature corresponding to the peak in the differential thermogravimetric traces. [i] Crystallization temperature. [j] Melting temperature.

underwent an irreversible reduction originating from the quinoxaline segment.[17] The reduction potential is more negative than those observed for the simple quinoxaline derivatives,[21] which indicates the electron-donating role of the indole unit. No oxidation wave was noticed within the observable potential window. LUMO values were calculated from the reduction potentials by comparing with the ionization potential of ferrocene (LUMO = 4.8 − E_{red}; where E_{red} is the reduction potential of the material with reference to ferrocene) and the HOMO values subsequently deduced from the band gap obtained from the optical edge. The data are listed in Table 3. The orbital energy values are favorable for charge injection and transport in a multilayered OLED configuration. The similar HOMO and LUMO levels observed for the dyes are in keeping with the expectation as they possess similar structural elements, and the peripheral Müllen dendrons are not expected to play a pronounced electronic role. The HOMO and LUMO energy levels observed for the dyes are comparable to the commonly used electron-transport materials such as tris(8-quinolinolate)Al(III) (Alq_3)[26] (−6.0 eV, −3.0 eV) and 1,3,5-tris(*N*-phenyl-benzimidizol-2-yl)benzene (TPBI)[27] (−6.2 eV, −2.7 eV).

Thermal Properties. Thermal stability of the materials was investigated by thermogravimetric analyses (TGA). All of the materials showed very good thermal stability. The onset decomposition temperatures of the compounds lie in the range from 363 to 465 °C (Table 3). In general, the onset temperatures of compounds **3a**−**5a** are smaller than those of the analogous compounds **3b**−**5b** containing an extra phenyl group. This means that the phenyl substituted compounds **3b**−**5b** resist decomposition. Irrespective of the variation in the onset temperatures, the more or less comparable decomposition temperatures observed for the dyes indicate that the thermal robustness of the compounds primarily arises from the indoloquinoxaline segment. Müllen dendrons containing pyrenylamine substituents and related derivatives have been demonstrated to function as hole-transporting and emitting materials in organic light-emitting diodes possessing relatively low thermal decomposition temperatures (296−456)[10] when compared to the materials studied in this work. Insertion of indolo[3,2-*b*]quinoxaline as core highly benefits the thermal decomposition temperature of these materials and raises them to 480−496 °C. It may be attributed to the planar nature of the indolo[3,2-*b*]quinoxaline moiety, which provides additional thermal stability. The glass-forming capability of the dyes was examined by differential scanning calorimetry. Compounds **3a**, **3b**, **4a**, and **5b** exhibited glass transition temperatures (T_g) in the range 103−156 °C. These values are significantly larger than those reported earlier for triarylamines-substituted indoloquinoxalines[13] and that of commonly used hole-transporting agents such as 1,4-bis(phenyl-*m*-tolylamino)biphenyl (TPD, T_g = 60 °C) and 4,4′-bis(1-naphthylphenylamino)biphenyl (NPB, T_g = 95 °C).[28] The pronounced stability of the glassy state in these molecules is attributable to the presence of indoloquinoxaline and other polyaromatic hydrocarbons such as fluoranthene and triphenylene. The additional phenyl

dx.doi.org/10.1021/jo2004764 |*J. Org. Chem.* 2011, 76, 4571–4581

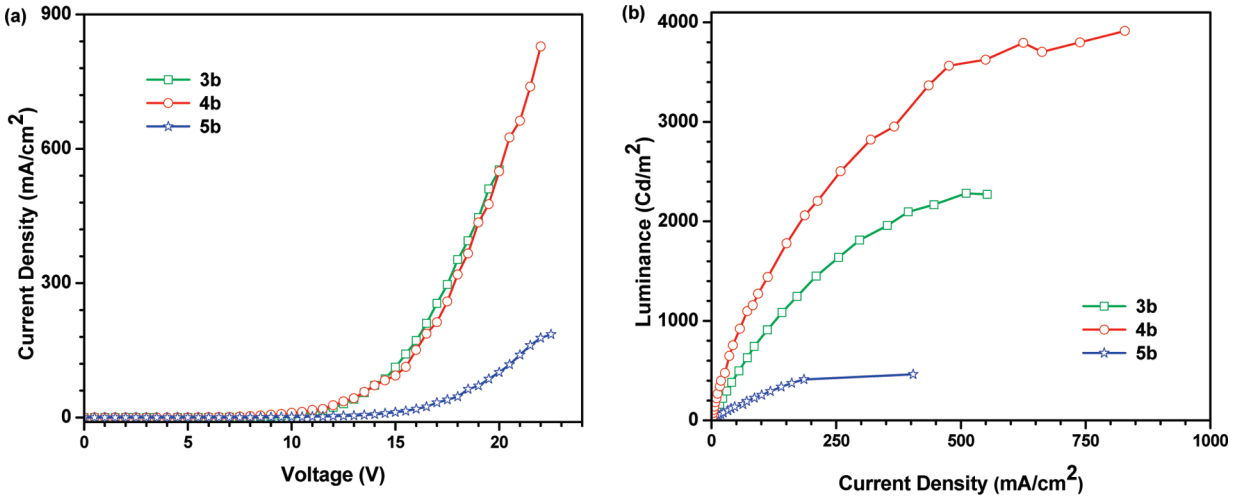

Figure 7. EL characters of the device with the structure ITO/NPB/**3b**−**5b**/Al (device I): (a) current density−voltage (I−V); (b) luminance−voltage (L−V) curves.

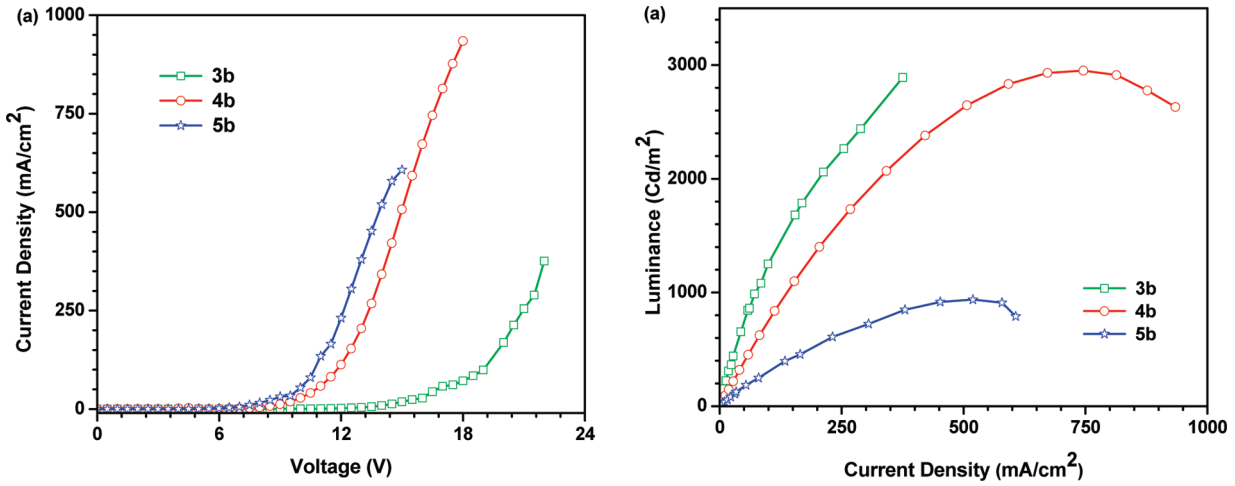

Figure 8. EL characters of device with the structure ITO/NPB/**3b**−**5b**/TPBI/Al (device II): (a) current density−voltage (I−V); (b) luminance−voltage (L−V) curves.

Table 4. EL Parameters for the Devices Fabricated Using Compounds 3b−5b

compd		V_{on}, V[a]	λ_{em}, nm	CIE (x, y)	fwhm, nm[b]	L_{max}, cd/m^2[c]	L, cd/m^2[d]	η_v, %[e]	η_p, lm/W[f]	η_c, cd/A[g]
3b	Device I	14.8	498	0.21, 0.46	80	2280	832	0.315	0.178	0.836
	Device II	19.1	496	0.19, 0.45	78	2890	1256	0.476	0.208	1.257
4b	Device I	15.2	504	0.23, 0.51	82	3910	1329	0.455	0.276	1.333
	Device II	11.8	496	0.20, 0.39	86	2950	750	0.321	0.200	0.751
5b	Device I	20.0	516	0.23, 0.62	76	740	253	0.075	0.040	0.253
	Device II	10.9	454	0.20, 0.24	138	940	304	0.198	0.090	0.306

[a] Turn-on voltage. [b] Full width at half-maximum. [c] Maximum luminance. [d] Luminance at 100 mA/cm^2. [e] External quantum efficiency. [f] Power efficiency at 100 mA/cm^2. [g] Current efficiency at 100 mA/cm^2.

group present in **3b** is also helpful to increase T_g when compared to the analogue **3a**.

Electroluminescent Characteristics. To evaluate the performance of novel 6*H*-indolo[3,2-*b*]quinoxaline based Müllen dendrons as a constituent in organic light-emitting diodes we have first attempted devices having ITO/**3b**−**5b**/Al where the compounds served as emissive and dual charge transporting materials. However, no significant light emission was observed even at higher operating voltages. This is quite expected as the compounds lack hole-transporting segments such as amines. So we have turned our attention to use them as emitting/electron transporting materials. Thus, we have fabricated two types of devices with the structures ITO/NPB/**3b**−**5b**/Al (device I) and ITO/NPB/**3b**−**5b**/TPBI/Al (device II) where

dx.doi.org/10.1021/jo2004764 |*J. Org. Chem.* 2011, 76, 4571–4581

NPB is *N*,*N*′-diphenyl-*N*,*N*′-bis(1-naphthylphenyl)-1,1′-biphenyl-4,4′-diamine serving as the hole-transporting layer and TPBI is 1,3,5-tris(*N*-phenylbenzimidizol-2-yl)benzene acting as an electron-transporting material. The compounds were spin-coated on the NPB layer, and a TPBI layer was deposited on the top of it to achieve the device II. In the device II, the 6*H*-indolo[3,2-*b*]quinoxaline based Müllen dendrons act as emissive layer, whereas in device I, they act as electron-transporting layer as well as emitting layer.

The current density−voltage (I−V) and luminance−current density (L−I) characteristics of the OLEDs fabricated using these dyes are shown in Figure 7 and 8 respectively. The device performance and EL emission characteristics are summarized in Table 4. In the device configuration I, the lower current density and larger turn-on voltage was observed for the diode fabricated using **5b** while for configuration II these parameters were realized for **3b**. It appears that **5b** lacks electron-transporting ability and inclusion of electron-transporting layer derived from TPBI improves the current flow in the device. On the contrary for **3b** addition of TPBI layer probably inhibits the electron injection into the molecular layer and reduces the current density. For **4b** addition of TPBI layer is beneficial for the electroluminescence performance. Some of these observations may be rationalized by looking at the energy alignments for the device configurations shown in Figure 9. Holes leaking to **4b**/**5b** is less favorable when compared to **3b** due to higher energy barrier at the **4b**,**5b**/TPBI interface. Similarly a barrier of 0.1 eV is there for the injection of electrons into the **3b** layer from TPBI. In the case of **5b** despite an improvement in the current density and turn-on voltage with additional TPBI layer, the luminance drastically decreased due to the exciplex formation between TPBI and **5b** and the confinement of charge recombination of zone comprising of TPBI layer (see below).

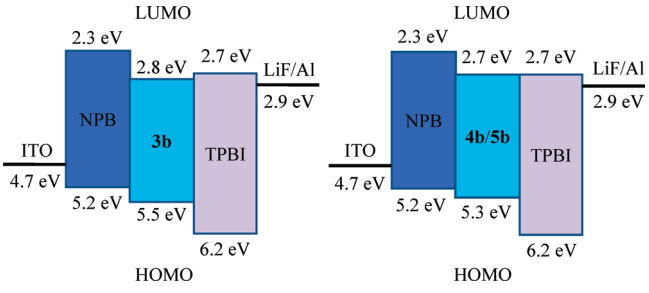

Figure 9. Orbital energy alignments in the molecular materials used in this study.

The emission in both the devices originates from the indoloquinoxaline derivatives to give bluish-green or green color depending on the dye used (Figure 10). As can be seen in Figure 10, λ_{max} (∼490−520 nm) of the EL spectra is about 10−20 nm red-shifted when compared to that of the PL spectrum of the solid film (shown in Figure 4). The EL spectra (Figure 10a) for the devices made from compound **5b** containing TPBI (device II), are characteristic of contamination of emission from TPBI or exciplex indicating the formation of excitons at the interface of TPBI/**5b** layers. On the contrary the device where compound **5b** is acting as an electron transport layer and emitter (device I), the emission peak is centered at 520 nm (Figure 10b). This may be due to the excimer formation of **5b**.[29] The compound **5b** is already demonstrated to form excimers in toluene solutions and spin-coated thin films (*vide supra*).

Among the compounds (**3b**−**5b**), that containing the fluoranthene skeleton, **4b**, displays larger current density at higher voltages. The turn-on voltage of compound **4b** in device II was 11.8 V and it exhibited bluish-green EL (CIE: 0.20, 0.39) with a maximum brightness of 2950 cd/m^2 at 16.5 V and a maximum efficiency of 0.32%. A device II of fluoranthene derivative, **4b** showed better characteristics with the turn-on voltage of 15.2 V, a maximum brightness of 3910 cd/m^2 at 18.7 V, and a maximum efficiency of 0.46%. However, **3b** as emitting material displayed a bluish-green electroluminescence (CIE: 0.19, 0.45) of 2890 cd/m^2 and maximum external quantum efficiency of 0.48%. On the other hand, the device fabricated using a layer of **3b** as electron transporting and emitting material has shown inferior current−voltage-luminance characteristics (maximum luminescence 2280 cd/m^2 and maximum external quantum efficiency of 0.32%). In short, inclusion of an electron-transport layer of TPBI benefits the device performance for **3b** however decrements the luminance characteristics for **4b**. Thicker layer of **4b** probably reduces the chances of electrons leaking into the NPB layer by retarding their movement, while the addition of facile electron-transport TPBI enhances the possibility of electron-leaking into the NPB and spreading the recombination zone inside the NPB

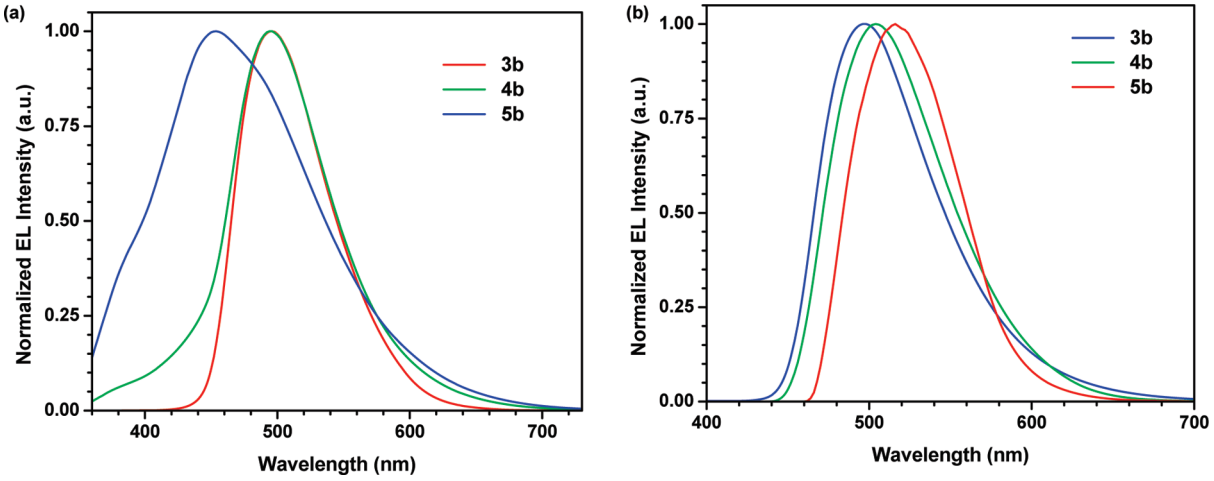

Figure 10. EL spectra observed for (a) device II and (b) device I using compounds **3b**−**5b** as emitters/electron transporters.

layer. Thus for **4b** in device II residual emission from NPB is also observed (see Figure 10a).

CONCLUSIONS

In summary, we have demonstrated that Müllen dendron-like chromophores attached to an indoloquinoxaline core is an effective structural skeleton for improving thermal properties. They were easily synthesized by performing a Diels−Alder reaction between the acetylene derivatives and appropriate cyclopentadienones. We have investigated their electrochemical, photophysical, and electroluminescence properties. All of the novel compounds display good quantum yields in solutions and also show remarkable fluorescence in the solid state. They displayed irreversible electrochemical reduction, demonstrating their electron-accepting nature. In accordance with these results they reasonably functioned as emitting material or as emitting and electron-transporting material in multilayered organic light-emitting diodes. Two types of multilayered device were fabricated, using these materials as the electron-transporting and/or emitting layers. Both the devices exhibited moderate performance. An OLED device fabricated using a layer of **4b** as electron-transporting and emitting material displayed a maximum luminescence of 3910 cd/m^2 and maximum external quantum efficiency of 0.46%, whereas the device fabricated using a layer of **4b** as emitting material along with a TPBI electron-transporting layer slightly reduced the device performance parameters (maximum luminescence 2950 cd/m^2 and maximum external quantum efficiency of 0.32%). Incorporation of an additional layer of TPBI is detrimental to the device function, which probably indicates the retardation of electron injection into the molecular layer of **4b** from the TPBI layer. These results reveal that the newly developed materials are good electron-transporting as well as emitting materials suitable for double layer organic light-emitting diodes.

EXPERIMENTAL SECTION

General. ^{1}H and ^{13}C NMR spectra were recorded on a spectrometer operating at 500 MHz. Mass spectra were collected on an ESI TOF high-resolution mass spectrometer. Electronic absorption spectra were measured on a spectrophotometer using dichloromethane or toluene solutions. Emission spectra were recorded using a spectrofluorimeter operating at room temperature (~30 °C). Emission quantum yields were obtained by using coumarin-6 (Φ_F = 0.78 in ethanol) as reference. Cyclic voltammetric experiments were performed using an electrochemical analyzer with a conventional three-electrode configuration consisting of a glassy carbon working electrode, platinum auxiliary electrode, and a nonaqueous Ag/AgNO$_3$ reference electrode. The $E_{1/2}$ values were determined as $1/2(E^p_a + E^p_c)$, where E^p_a and E^p_c are the anodic and cathodic peak potentials, respectively. All potentials reported are referenced to ferrocene, which served as the internal standard. The solvent in all experiments was CH_2Cl_2, and the supporting electrolyte was 0.1 M tetrabutylammonium hexafluorophosphate. DSC measurements were carried out on a differential scanning calorimeter at a heating rate of 10 °C/min and a cooling rate of 30 °C/min under nitrogen atmosphere. Melting temperatures of the compounds were obtained from the DSC measurements. The decomposition temperatures are reported as the melting points for the dyes that did not exhibit a melting exotherm in the DSC trace. TGA measurements were performed on a thermogravimetric analyzer at a heating rate of 10 °C/min under a flow of air.

The precursors 2,3,4,5-diphenylcyclopenta-2,4-dienone,[10] 7,9-diphenyl-8*H*-cyclopenta[*a*]acenaphthylen-8-one,[30] 1,3-diphenyl-2*H*-cyclopenta[l]phenanthren-2-one[31] and 9-bromo-6-butyl-6*H*-indolo[3,2-*b*]-quinoxaline[13] were prepared by following literature procedures.

6-Butyl-9-ethynyl-6H-indolo[3,2-b]quinoxaline (***2b***). 9-Bromo-6-butyl-6*H*-indolo[3,2-*b*]quinoxaline (**1b**, 1.06 g, 3.0 mmol), Pd(PPh$_3$)$_2$Cl$_2$ (0.035 g, 0.03 mmol), CuI (0.005 g, 0.09 mmol), PPh$_3$ (0.026 g, 0.03 mmol), 2-methylbut-3-yn-2-ol (0.3 g, 3.6 mmol), and triethylamine (50 mL) were charged sequentially in a two-neck flask under nitrogen atmosphere and heated to reflux for 12 h. The volatiles were removed under vacuum, and the resulting solid was extracted into diethyl ether. The organic extract was washed with brine solution, dried over anhydrous Na$_2$SO$_4$, and evaporated to leave a pale green solid. It was further purified by column chromatography on silica gel using dichloromethane as eluant to obtain 4-(6-butyl-6*H*-indolo[3,2-*b*]-quinoxalin-9-yl)-2-methylbut-3-yn-2-ol (**2a**) as a yellow solid 0.95 g (89%). ^{1}H NMR (500 MHz, CDCl$_3$) δ 0.98 (t, J = 7.3 Hz, 3 H), 1.42 (sext, J = 7.5 Hz, 3 H), 1.67 (s, 6 H), 1.92 (quin, J = 7.5 Hz, 2 H), 2.33 (s, 1 H), 4.47 (t, J = 7.3 Hz, 2 H), 7.38 (d, J = 8.5 Hz, 2 H), 7.67−7.69 (m, 2 H), 7.76 (td, J = 8.0 Hz, 1.25 Hz, 1 H), 8.13 (dd, J = 6.0 Hz, 1.0 Hz 1 H), 8.29 (dd, J = 9.5 Hz, 1.0 Hz, 1 H), 8.54 (d, J = 1.0 Hz, 1 H).

It was quantitatively converted into the 6-butyl-9-ethynyl-6*H*-indolo-[3,2-*b*]quinoxaline (**2b**) by treatment with refluxing solution of potassium hydroxide in toluene at 110 °C temperature for 6 h. Reaction mixture was extracted with diethyl ether and dried over Na$_2$SO$_4$. Yellow solid; yield 0.85 g (95%); ^{1}H NMR (500 MHz, CDCl$_3$) δ 0.99 (t, J = 7.5 Hz, 3 H), 1.46 (sext, J = 7.5 Hz, 3 H), 1.67 (s, 6 H), 1.92 (quin, J = 7.5 Hz, 2 H), 3.11 (s, 1 H), 4.49 (t, J = 7.5 Hz, 2 H), 7.41 (d, J = 8.5 Hz, 1 H), 7.66−7.69 (m, 1 H), 7.76 (td, J = 8.0 Hz, 1.25 Hz, 1 H), 8.13 (dd, J = 6.0 Hz, 1.5 Hz, 1 H), 8.14 (dd, J = 8.5 Hz, 1.5 Hz, 1 H), 8.30 (dd, J = 8.5 Hz, 1.3 Hz, 1 H), 8.63 (d, J = 2.0 Hz, 1 H); ^{13}C NMR (125 MHz, CDCl$_3$) δ 13.7, 20.3, 30.6, 41.4, 83.7, 100.0, 109.5, 114.4, 119.5, 126.2, 126.6, 127.9, 129.0, 129.4, 134.5, 139.2, 139.4, 140.7, 144.1, 145.8; HRMS calcd for $C_{20}H_{17}N_3$ m/z 299.1422, found 299.1429.

6-Butyl-9-(2-phenylethynyl)-6H-indolo[3,2-b]quinoxaline (***2c***). 9-Bromo-6-butyl-6*H*-indolo[3,2-*b*]quinoxaline (**1b**) (1.06 g, 3.0 mmol), Pd(PPh$_3$)$_2$Cl$_2$ (0.035 g, 0.03 mmol), CuI (0.005 g, 0.09 mmol), PPh$_3$ (0.026 g, 0.03 mmol), phenylacetylene (0.34 g, 6.0 mmol), and diisopropylamine (40 mL) were charged sequentially into a two-neck flask under nitrogen atmosphere and heated to reflux for 24 h. After the stipulated time, the volatiles were removed under vacuum, and the resulting solid was extracted into ethyl acetate. The organic extract was washed with brine solution, dried over anhydrous Na$_2$SO$_4$, and evaporated to leave a yellow solid. It was further purified by column chromatography using CH_2Cl_2 and *n*-hexane (2:3) mixture. Yellow solid; yield 1.06 g (94%); ^{1}H NMR (500 MHz, CDCl$_3$) δ 0.99 (t, J = 7.3 Hz, 3 H), 1.45 (sext, J = 7.8 Hz, 2 H), 1.94 (quin, J = 7.5 Hz, 2 H), 4.51(t, J = 7.5 Hz, 2 H), 7.35−7.40 (m, 3 H), 7.43 (d, J = 8.5 Hz, 1 H), 7.57−7.59 (m, 2 H), 7.69 (td, J = 5.8 Hz, 1 Hz, 1 H), 7.77 (td, J = 5.8 Hz, 1.0 Hz, 1 H), 7.85 (dd, J = 8.5 Hz, 1.5 Hz, 1 H), 8.15 (d, J = 8.5 Hz, 1 H), 8.31 (d, J = 8.0 Hz, 1 H), 8.68 (s, 1 H); ^{13}C NMR (125 MHz, CDCl$_3$) δ 13.7, 20.2, 30.4, 41.3, 88.6, 89.4, 109.5, 110.9, 113.4, 115.5, 119.5, 121.0, 123.4, 126.0, 126.0, 126.1, 127.8, 128.0, 128.3, 128.8, 129.0, 129.4, 131.4, 133.2, 133.9, 138.6, 139.3, 139.3, 140.6, 142.8; HRMS calcd for $C_{26}H_{21}N_3$ m/z 375.1735, found 375.1722.

Compound ***3a***. A mixture of 2,3,4,5-tetraphenylcyclopenta-2,4-dienone (0.58 g, 1.5 mmol), **2b** (0.50 g, 1.65 mmol) and diphenyl ether (5 mL) were heated under nitrogen atmosphere at 200 °C for 24 h during which the dark purple color vanished and an orange color developed. After cooling, hexane was added to precipitate the product formed. The yellow color precipitates formed was filtered and dried under vacuum. Further purification of the crude product was performed by column chromatography on silica gel and using hexane−dichloromethane mixture (1:1) as eluant. Yellow solid; yield 92%; mp 400 °C (dec); ^{1}H NMR (500 MHz, CDCl$_3$) δ 1.29

dx.doi.org/10.1021/jo2004764 |J. Org. Chem. 2011, 76, 4571–4581

(t, J = 7.5 Hz, 3 H), 1.71−1.76 (m, 2 H), 2.2−2.23 (m, 2 H), 4.75 (t, J = 7.25 Hz, 2 H), 7.16−7.28 (m, 12 H), 7.45−7.53 (m, 7 H), 7.58 (s, 1 H), 7.25 (dd, J = 1.0 Hz, 8.5 Hz, 2 H), 7.98 (t, J = 7.0 Hz, 1 H), 8.05−8.08 (m, 3 H), 8.44 (d, J = 8.5 Hz, 1 H), 8.59 (d, J = 8.5 Hz, 1 H), 8.85 (s, 1 H); ^{13}C NMR (125 MHz, $CDCl_3$) δ 13.8, 20.3, 29.7, 30.6, 41.3, 123.7, 125.4, 125.7, 125.7, 125.8, 126.3, 126.7, 127.0, 127.1, 127.6, 129.4, 129.9, 131.5, 131.6, 131.8, 132.0, 133.3, 134.7, 139.3, 139.3, 139.3, 140.0, 140.1, 140.2, 140.2, 140.4, 140.6, 141.1, 141.7, 141.9, 143.1, 145.9; HRMS calcd for $C_{48}H_{38}N_3$ [M + H] m/z 656.3066, found 656.3099. Anal. Calcd for $C_{48}H_{37}N_3$: C, 87.91; H, 5.69; N, 6.41. Found: C, 87.80; H, 5.76; N, 6.37.

Compound ***4a***. Synthesized from 7,9-diphenyl-8*H*-cyclopenta-[*a*]acenaphthylen-8-one and **2b** by following the procedure described above for **3a**: yellow solid; yield 95%; mp 303 °C; ^{1}H NMR (500 MHz, $CDCl_3$) δ 0.95−0.99 (m, 3 H), 1.26−1.4 (m, 2 H), 1.56−1.57 (m, 2 H), 4.47 (t, J = 7.25 Hz, 2 H), 6.71−6.72 (m, 1 H), 7.21−7.22 (m, 1 H), 7.31−7.59 (m, 14 H), 7.66 (t, J = 8.0 Hz, 1 H), 7.73−7.77 (m, 5 H), 7.76 (d, J = 8.5 Hz, 1 H), 8.28 (d, J = 9.0 Hz, 1 H), 8.51 (s, 1 H). ^{13}C NMR (125 MHz, $CDCl_3$) δ 13.8, 20.3, 29.7, 30.6, 41.3, 108.4, 119.2, 123.0, 123.4, 123.7, 125.8, 126.7, 126.7, 127.4, 127.6, 127.7, 127.8, 127.9, 128.7, 128.7, 129.2, 129.4, 130.5, 131.7, 133.2, 134.0, 135.8, 136.0, 136.3, 136.7, 138.2, 138.3, 139.3, 139.4, 140.2, 140.3, 140.6, 140.8, 143.1, 145.9. HRMS calcld for $C_{46}H_{34}N_3$ [M + H] m/z 628.2753, found 628.2833. Anal. Calcd for $C_{46}H_{33}N_3$: C, 88.01; H, 5.30; N, 6.69. Found: C, 87.88; H, 5.38; N, 6.61.

Compound ***5a***. Synthesized from 1,3-diphenyl-2*H*-cyclopenta-[l]phenanthren-2-one and **2b** by following the procedure described above for **3a**: yellow solid; yield 72%; mp 359 °C; ^{1}H NMR (500 MHz, $CDCl_3$) δ 0.98 (t, J = 7.25 Hz, 3 H), 1.25 (sext, J = 7.5 Hz, 2 H), 1.93 (q, J = 7.5 Hz, 2 H), 4.46 (t, J = 7.25 Hz, 2 H), 7.01−7.02 (m, 2 H), 7.08−7.12 (m, 2 H), 7.18−7.19 (m, 5 H), 7.38−7.56 (m, 6 H), 7.52−7.56 (m, 3 H), 7.65 (t, J = 8.5 Hz, 1 H), 7.65−7.78 (m, 2 H), 7.84 (s, 1 H), 8.13 (d, J = 8.5 Hz, 1 H), 8.26 (d, J = 8.5 Hz, 1 H), 8.45 (d, J = 8.5 Hz, 2 H), 8.52 (s, 1 H); ^{13}C NMR (125 MHz, $CDCl_3$) δ 145.9, 144.4, 143.0, 142.2, 140.6, 140.1, 139.7, 139.3, 138.4, 136.6, 134.6, 133.2, 133.0, 132.3, 132.0, 131.7, 131.4, 130.8, 130.2, 130.1, 130.0, 129.8, 129.7, 129.6, 129.4, 129.1, 128.7, 128.6, 127.8, 127.2, 126.7, 126.4, 125.9, 125.6, 125.3, 123.5, 123.3, 123.2, 119.4, 118.9, 108.5, 41.3, 31.0, 30.6, 20.3, 13.8; HRMS calcld for $C_{48}H_{36}N_3$ [M + H] m/z 654.2909, found 654.2914. Anal. Calcd for $C_{48}H_{35}N_3$: C, 88.18; H, 5.40; N, 6.43. Found: C, 88.22; H, 5.34; N, 6.36.

Compound ***3b***. Synthesized from 2,3,4,5-tetraphenylcyclopenta-2,4-dienone and **2c** by following the procedure described above for **3a**: yellow solid; yield 1.0 g (91%); mp 319 °C; ^{1}H NMR (500 MHz, $CDCl_3$) δ 0.91 (t, J = 7.5 Hz, 3 H), 1.29 (m, 2 H), 1.66 (m, 2 H), 4.30 (t, J = 7.5 Hz, 2 H), 6.70−6.73 (m, 2 H), 6.76−6.93 (m, 23 H), 6.98 (d, J = 8.5 Hz, 1 H), 7.19 (dd, J = 8.5 Hz, 1.5 Hz 1 H), 7.61 (td, J = 8.5 Hz, 1.5 Hz, 1 H) 7.69 (td, J = 8.5 Hz, 1.5 Hz, 1 H), 7.96 (dd, J = 1.5 Hz, 1 H), 8.05 (dd, J = 8.0 Hz, 1.25 Hz, 1 H), 8.20 (dd, J = 8.0 Hz, 1.25 Hz, 1 H). ^{13}C NMR (125 MHz, $CDCl_3$) δ 13.8, 20.2, 30.4, 41.2, 107.8, 118.2, 125.1, 125.2, 125.4, 125.5, 126.5, 126.6, 126.7, 126.8, 127.7, 128.4, 129.2, 131.3, 131.4, 131.5, 131.7, 133.7, 134.3, 139.1, 140.35, 140.39, 140.43, 140.46, 140.59, 140.64, 140.8, 142.3, 145.8. FABMS m/z 732 [M + H]; HRMS calcd for $C_{54}H_{42}N_3$ [M + H] m/z 732.3379, found 732.3392. Anal. Calcd for $C_{54}H_{41}N_3$: C, 88.61; H, 5.65; N, 5.74. Found: C, 88.72; H, 5.54; N, 5.78.

Compound ***4b***. Synthesized from 7,9-diphenyl-8*H*-cyclopenta-[*a*]acenaphthylen-8-one and **2c** by following the procedure described above for **3a**: greenish yellow solid; yield 92%; mp 460 °C (dec); ^{1}H NMR (500 MHz, $CDCl_3$) δ 0.90 (t, J = 7.5 Hz, 3 H), 1.26−1.33 (m, 2 H), 1.80 (quin, J = 7.0 Hz, 2 H), 4.30 (t, J = 7.0 Hz, 2 H), 6.60 (d, J = 7.0 Hz, 1 H), 6.64 (d, J = 7.0 Hz, 1 H), 6.80 (t, J = 7.0 Hz, 1 H), 6.84 (t, J = 7.0 Hz, 1 H), 6.96 (d, J = 7.5 Hz, 1 H), 7.01 (d, J = 8.0 Hz, 2 H), 7.17 (t, J = 7.5 Hz, 1 H), 7.28−7.44 (m, 9 H), 7.43 (d, J = 7.5 Hz, 1 H), 7.61 (t, J = 7.5 Hz, 1 H), 7.63−7.73 (m, 3 H), 8.05−8.07 (m, 2 H), 8.24 (d, J = 8.0 Hz, 1 H); ^{13}C NMR (125 MHz, $CDCl_3$) δ 13,7, 20.1, 39.5, 40.2, 107.8, 118.2, 123.2, 123.3, 125.2, 125.4, 125.6, 126.6, 126.86, 126.89, 126.91, 127.7, 128.1, 128.3, 128.4, 128.5, 129.2, 129.7, 129.8, 130.0, 130.2, 130.4, 131.1, 131.6, 132.9, 133.3, 134.2, 136.6, 136.6, 137.3, 137.7, 139.1, 139.9, 140.2, 140.3, 140.5, 141.2, 142.4; FABMS m/z 704 [M + H]; HRMS calcd for $C_{52}H_{38}N_3$ [M + H] m/z 704.3066, found 704.3081. Anal. Calcd for $C_{52}H_{37}N_3$: C, 88.73; H, 5.30; N, 5.97. Found: C, 88.81; H, 5.24; N, 5.89.

Compound ***5b***. Synthesized from 1,3-diphenyl-2*H*-cyclopenta-[l]phenanthren-2-one and **2c** by following the procedure described above for **3a**: yellow solid; yield 60%; mp 465 °C (dec); ^{1}H NMR (500 MHz, $CDCl_3$) δ 0.94 (t, J = 7.5 Hz, 3 H), 1.31 (sext, J = 7.5 Hz, 2 H), 1.84 (quin, J = 7.5 Hz, 2 H), 4.36 (t, J = 7.25 Hz, 2 H), 6.71−6.83 (m, 5 H), 6.98−7.10 (m, 14 H), 7.42 (q, J = 8.25 Hz, 1 H), 7.60−7.64 (m, 3 H), 7.70 (td, J = 7.5 Hz, 1.5 Hz, 1 H), 8.08 (dd, J = 8.25 Hz, 1.03 Hz, 1 H), 8.20 (dd, J = 8.5 Hz, 1.0 Hz 1 H), 8.44 (d, J = 8.0 Hz, 1 H); ^{13}C NMR (125 MHz, $CDCl_3$) δ 13.8, 20.2, 30.4, 41.2, 107.9, 118.3, 123.2, 125.2, 125.4, 125.6, 126.1, 126.2, 126.4, 126.5, 126.9, 127.9, 128.0, 128.3, 128.4, 129.3, 130.0, 130.1, 130.8, 130.9, 131.3, 131.36, 131.39, 131.6, 131.9, 132.0, 132.1, 132.2, 132.4, 133.3, 134.4, 137.2, 137.6, 139.1, 140.0, 140.30, 140.34, 140.5, 140.9, 142.4; FABMS m/z 730 [M + H]; HRMS calcd for $C_{54}H_{40}N_3$ [M + H] m/z 730.3222, found 730.3243. Anal. Calcd for $C_{54}H_{39}N_3$: C, 88.86; H, 5.39; N, 5.76. Found: C, 88.75; H, 5.47; N, 5.81.

Light-Emitting Diode Fabrication and Characterization. Prepatterned ITO substrates with an effective individual device area of 3.14 mm^2 were cleaned *via* repeated ultrasonic washing with detergent, deionized water, ethanol and finally oxygen plasma treatment. A layer of *N*,*N*′-bis(l-naphthyl)-*N*,*N*′-diphenyl-1,1′-biphenyl-4,4′-diamine (NPB) with a thickness of 40 nm was vacuum-deposited on the precleaned ITO glass substrates as a hole-transport layer and then baked at 100 °C in air for 1 h. Then, the indoloquinoxaline derivative (**3b**, **4b**, or **5b**) was dissolved in dichlorobenzene (concentration 10 mg mL^{-1}) and filtered with a 0.2 mm filter. A thin film of the desired material (**3b**/**4b**/**5b**) was coated at a spin rate of 1500 rpm. The film thickness of this layer was around 40 nm, measured by a surface profilometer Dektak 3 (Veeco/Sloan Instrument Inc.) for device I and 10 nm for device II. Finally, a layer of LiF/Al (1 nm/120 nm) was thermally evaporated as a cathode in a vacuum chamber (under a pressure of less than 2.5 × 10^{-5} Torr). For device II, a layer (with a thickness of 30 nm) of electron-transporting 1,3,5-tris(*N*-phenylbenzimidazol-2-yl)benzene (TPBI) was deposited under vacuum before the deposition of LiF/Al layer. I−V curves were measured on a Keithley 2400 Source Meter in ambient environment, and the light intensity was measured with a Newport 1835 Optical Meter.

Computational Methods. The ground state geometry of the compounds at the gas phase were optimized using the density functional theory method with the B3LYP functional[32] in conjugation with the basis set 6-31G(d,p) as implemented in the Gaussian 09 package. The default options for the self-consistent field (SCF) convergence and threshold limits in the optimization were used. The optimized structures did not show imaginary frequency vibrations. The electronic transitions were calculated using the time-dependent DFT (B3LYP) theory and the 6-31G (d,p) basis set. Even though the time-dependent DFT method less accurately describes the states with charge-transfer nature, the qualitative trends in the TDDFT results can still offer correct physical insights. At least 10 excited states were calculated for each molecule.

■ ASSOCIATED CONTENT

Supporting Information. Absorption and emission spectra, ^{1}H and ^{13}C NMR of the newly synthesized compounds, and Cartesian coordinates of the optimized structures. This material is available free of charge via the Internet at http://pubs.acs.org.

AUTHOR INFORMATION

Corresponding Author

*Phone: +91-1332-285376. FAX: +91-1332-286202. E-mail: krjt8fcy@iitr.ernet.in.

ACKNOWLEDGMENT

We thank the Department of Science and Technology (DST), New Delhi, India for financial support (Grant No. SR/S1/OC-11/2007) and Prof. J. T. Lin, Institute of Chemistry, Academia Sinica, Taipei, Taiwan for his assistance in the fabrication and characterization of electroluminescent devices. Prof. R. Barthwal of the Department of Biotechnology is thanked for allowing us to use the NMR facility in the Institute Instrumentation Centre.

REFERENCES

(1) (a) Noine, K.; Pu, Y.-J.; Nakayama, K.-I.; Kido, J. *Org. Electron.* **2010**, *11*, 717. (b) Kwon, Y. S.; Lee, K. H.; Young, K. G.; Seo, J. H.; Kim, Y. K.; Yoont, S. S. *J. Nanosci. Nanotechnol.* **2009**, *9*, 7056. (c) Jiang, Z.; Liu, Z.; Yang, C.; Zhong, C.; Qin, J.; Yu, G.; Liu, Y. *Adv. Funct. Mater.* **2009**, *19*, 3987. (d) Lai, M.-Y.; Chen, C.-H.; Huang, W.-S.; Lin, J. T.; Ke, T.-H.; Chen, L.-Y.; Tsai, M.-H.; Wu, C.-C. *Angew. Chem., Int. Ed.* **2008**, *47*, 581. (e) Gao, Z. Q.; Li, Z. H.; Xia, P. F.; Wong, M. S.; Cheah, K. W.; Chen, C. H. *Adv. Funct. Mater.* **2007**, *17*, 3194. (f) Li, Z. H.; Wong, M. S.; Tao, Y.; Lu, J. *Eur. J. Chem.* **2005**, *11*, 3285. (g) Ego, B. C.; Grimsdale, F. U.; Yu, G.; Srdanov, G.; Müllen, K. *Adv. Mater.* **2002**, *14*, 809. (h) Loy, D. E.; Koene, B. E.; Thompson, M. E. *Adv. Func. Mater.* **2002**, *12*, 245.

(2) (a) Nakanishi, W.; Hitosugi, S.; Piskareva, A.; Shimada, Y.; Taka, H.; Kita, H.; Isobe, H. *Angew. Chem., Int. Ed.* **2010**, *49*, 7239. (b) Gong, M. S.; Lee, H. S.; Jeon, Y. M. *J. Mater. Chem.* **2010**, *20*, 10735. (c) Kim, S. K.; Yang, B.; Park, Y.-I.; Ma, Y.; Lee, J.-Y.; Kim, H.-J.; Park, J. *Org. Electron* **2009**, *10*, 822. (d) Yang, B.; Kim, S. K.; Xu, H.; Park, Y.-I.; Zhang, H.-Y.; Gu, C.; Shen, F. Z.; Wang, C. L.; Liu, D. D.; Liu, X. D.; Hanif, M.; Tang, S; Li, W. J.; Li, F.; Shen, J. C.; Park, J. W.; Ma, Y.-G. *ChemPhysChem* **2008**, *9*, 2601. (e) Yu, M. X.; Duan, J. P.; Lin, C. H.; Cheng, C. H.; Tao, Y. T. *Chem. Mater.* **2002**, *14*, 3958.

(3) (a) Sonar, P.; Soh, M.-S.; Cheng, Y.-H.; Henssler, J. T.; Sellinger, A. *Org. Lett.* **2010**, *12*, 3292. (b) Jia, W.-L.; McCormick, T.; Liu, Q.-D.; Fukutani, H.; Motala, M.; Wang, R.-Y.; Tao, Y.; Wang, S. *J. Mater. Chem.* **2004**, *14*, 3344.

(4) (a) Tasios, N.; Grigoriadis, C.; Hansen, M. R.; Wonneberger, H.; Li, C.; Spiess, H. W.; Müllen, K.; Floudas, G. *J. Am. Chem. Soc.* **2010**, *132*, 7478–7487. (b) Avlasevich, Y.; Li, C.; Müllen, K. *J. Mater. Chem.* **2010**, *20*, 3814–3826. (c) Shen, W.-J.; Dodda, R.; Wu, C.-C.; Wu, F.-I.; Liu, T.-H.; Chen, H.-H.; Chen, C.-H.; Shu, C.-F. *Chem. Mater.* **2004**, *16*, 930. (d) Wu, C.-C.; Lin, Y.-T.; Chiang, H.-H.; Cho, T.-Y.; Chen, C.-W.; Wong, K.-T.; Liao, Y.-L.; Lee, G.-H.; Peng, S.-M. *Appl. Phys. Lett.* **2002**, *81*, 577.

(5) Freudenmann, R.; Behnisch, B.; Hanack, M. *J. Mater. Chem.* **2001**, *11*, 1618.

(6) (a) Kapoor, N.; Thomas, K. R. J. *New J. Chem.* **2010**, *24*, 2739. (b) Xia, Z. Y.; Su, J. H.; Fan, H. H.; Cheah, K. W.; Tian, H.; Che, C. H. *J. Phys. Chem. C* **2010**, *114*, 11602. (c) Tong, Q.-X.; Lai, S.-L.; Chan, M.-Y.; Zhou, Y.-C.; Kwong, H.-L.; Lee, C.-S.; Lee, S.-T.; Lee, T.-W.; Noh, T.; Kwon, O. *J. Phys. Chem. C* **2009**, *113*, 6227. (d) Yan, Q.; Zhou, Y.; Ni, B.-B.; Ma, Y.; Wang, J.; Pei, J.; Cao, Y. *J. Org. Chem.* **2008**, *73*, 5328.

(7) Zhou, Y.; He, Q.-G.; Yang, Y.; Zhong, H.-Z.; He, C.; Sang, G.-Y.; Liu, W.; Yang, C.-H.; Bai, F.-L.; Li, Y.-F. *Adv. Funct. Mater.* **2008**, *18*, 3299.

(8) (a) Pu, Y.-J.; Kamiya, A.; Nakayama, K.-I.; Kido, J. *Org. Electron* **2010**, *11*, 479. (b) Matsumoto, N.; Adachi, C. *J. Phys. Chem. C* **2010**, *114*, 4652.

(9) (a) Park, H.; Oh, D.; Park, J.-W.; Kim, J.-H.; Shin, S.-C.; Kim, Y.-H.; Kwon, S.-K. *Bull. Korean Chem. Soc.* **2010**, *31*, 1951. (b) Danel, K.; Huang, T.-H.; Lin, J. T.; Tao, Y.-T.; Chuen, C.-H. *Chem. Mater.* **2002**, *14*, 3860.

(10) Thomas, K. R. J.; Velusamy, M.; Lin, J. T.; Chuen, C. H.; Tao, Y. T. *J. Mater. Chem.* **2005**, *15*, 4453.

(11) Thomas, K. R. J.; Velusamy, M.; Lin, J. T.; Sun, S. S.; Tao, Y. T.; Chuen, C. H. *Chem. Commun.* **2004**, 2328.

(12) (a) Gregg, D. J.; Ollagnier, C. M. A.; Fittchet, C. M.; Draper, C. M. *Chem.—Eur. J.* **2006**, *12*, 3043. (b) Gao, P.; Cho, D.; Yang, X. Y.; Enkelmann, V.; Baumgarten, M.; Mullen, K. *Chem.—Eur. J.* **2010**, *16*, 5119.

(13) Thomas, K. R. J.; Tyagi, P. *J. Org. Chem.* **2010**, *75*, 8100.

(14) (a) Li, C.; Liu, M.; Pschirer, N. G.; Baumgarten, M.; Müllen, K. *Chem. Rev.* **2010**, *110*, 6817. (b) Schmaltz, B.; Weil, T.; Müllen, K. *Adv. Mater.* **2009**, *21*, 1067.

(15) (a) Chinchilla, R.; Nájera, C. *Chem. Rev.* **2007**, *107*, 874. (b) Sonogashira, K.; Tohda, Y.; Hagihara, N. *Tetrahedron. Lett.* **1975**, *16*, 4467.

(16) Thomas, K. R. J.; Lin, J. T.; Tao, Y.-T.; Chuen, C.-H. *Adv. Mater.* **2002**, *14*, 822.

(17) Thomas, K. R. J.; Lin, J. T.; Tao, Y.-T.; Chuen, C.-H. *Chem. Mater.* **2002**, *14*, 3852.

(18) Bergmann, P.; Paul, H. *Chem. Ber* **1967**, *100*, 828.

(19) Thomas, K. R. J.; Lin, J. T.; Tao, Y.-T.; Chuen, C.-H. *Chem. Mater.* **2004**, *16*, 5437.

(20) Thomas, K. R. J.; Lin, J. T.; Tao, Y.-T.; Chuen, C.-H. *Chem. Mater.* **2002**, *14*, 2796.

(21) (a) Bettenhausen, J.; Greczmiel, M.; Jandke, M.; Ströhriegl, P. *Synth. Met.* **1997**, *91*, 223. (b) Jandke, M.; Ströhriegl, P.; Berleb, S.; Werner, E.; Brütting, W. *Macromolecules* **1998**, *31*, 6434.

(22) (a) Kaafarani, B. R. *Chem. Rev.* **2011**, *23*, 378. (b) Kato, T.; Hirai, Y.; Nakaso, S.; Moriyama, M. *Chem. Soc. Rev.* **2007**, *36*, 1857. (c) Kumar, S. *Liq. Cryst.* **2004**, *32*, 1089.

(23) Liao, Y.-L.; Hung, W.-Y.; Hou, T.-H.; Lin, C. Y.; Wong, K.-T. *Chem. Mater.* **2007**, *19*, 6350.

(24) Frisch, M. J.; Trucks, G. W.; Schlegel, H. B.; Scuseria, G. E.; Robb, M. A.; Cheeseman, J. R.; Scalmani, G.; Barone, V.; Mennucci, B.; Petersson, G. A.; Nakatsuji, H.; Caricato, M.; Li, X.; Hratchian, H. P.; Izmaylov, A. F.; Bloino, J.; Zheng, G.; Sonnenberg, J. L.; Hada, M.; Ehara, M.; Toyota, K.; Fukuda, R.; Hasegawa, J.; Ishida, M.; Nakajima, T.; Honda, Y.; Kitao, O.; Nakai, H.; Vreven, T.; Montgomery, J. A., Jr.; Peralta, J. E.; Ogliaro, F.; Bearpark, M.; Heyd, J. J.; Brothers, E.; Kudin, K. N.; Staroverov, V. N.; Kobayashi, R.; Normand, J.; Raghavachari, K.; Rendell, A.; Burant, J. C.; Iyengar, S. S.; Tomasi, J.; Cossi, M.; Rega, N.; Millam, N. J.; Klene, M.; Knox, J. E.; Cross, J. B.; Bakken, V.; Adamo, C.; Jaramillo, J.; Gomperts, R.; Stratmann, R. E.; Yazyev, O.; Austin, A. J.; Cammi, R.; Pomelli, C.; Ochterski, J. W.; Martin, R. L.; Morokuma, K.; Zakrzewski, V. G.; Voth, G. A.; Salvador, P.; Dannenberg, J. J.; Dapprich, S.; Daniels, A. D.; Farkas, Ö .; Foresman, J. B.; Ortiz, J. V.; Cioslowski, J.; Fox, D. J. *Gaussian 09*, revision A.02; Gaussian, Inc.: Wallingford, CT, 2009.

(25) Ströhriegl, P.; Grazulevicius, J. V. *Adv. Mater.* **2002**, *14*, 1439.

(26) (a) Pohl, R.; Montes, V. A.; Shinar, J.; Anzenbacher, P. *J. Org. Chem.* **2004**, *69*, 1723. (b) Anderson, J. D.; McDonald, E. M.; Lee, P. A.; Anderson, M. L.; Ritchie, E. L.; Hall, H. K.; Hopkins, T.; Mash, E. A.; Wang, J.; Padias, A.; Thayumanavan, S.; Barlow, S.; Marder, S. R.; Jabbour, G. E.; Shaheen, S.; Kippelen, B.; Peyghambarian, N.; Wightman, R. M.; Armstrong, N. R. *J. Am. Chem. Soc.* **1998**, *120*, 9646.

(27) Ge, Z.; Hayakawa, T.; Ando, S.; Ueda, M.; Akiike, T.; Miyamoto, H.; Kajita, T.; Kakimoto, M.-A. *Chem. Mater.* **2008**, *20*, 2532.

(28) Koene, B. E.; Loy, D. E.; Thompson, M. E. *Chem. Mater.* **1998**, *10*, 2235.

(29) Yeh, H.-C.; Lee, R.-H; Chan, L.-H.; Lin, T.-Y. J.; Chen, C.-T.; Balasubramaniam, E; Tao, Y.-T. *Chem. Mater.* **2001**, *13*, 2788.

(30) Wehmeier, M.; Wagner, M.; Müllen, K. *Chem.—Eur. J.* **2001**, *7*, 2197.

(31) Wooi, G. Y.; White, J. M. *Org. Biomol. Chem.* **2005**, *3*, 972.

(32) Lee, C.; Yang, W.; Parr, R. G. *Phys. Rev. B* **1988**, *37*, 785.